Obrabotka metallov (tekhnologiya, oborudovanie, instrumenty) = Metal Working and Material Science. 2026 vol. 28 no. 1 pp. 193–206
ISSN: 1994-6309 (print) / 2541-819X (online)
DOI: 10.17212/1994-6309-2026-28.1-193-206

NSTU NETI

Obrabotka metallov - Metal Working and Material Science

Journal homepage: http://journals.nstu.ru/obrabotka_metallov

Dynamic modeling and selection of rational parameters for a millstone mill mechanism to reduce energy consumption

Yuriy Podgornyj [1, a, *], *Vladimir Ivancivsky* [1, b], *Tatyana Martynova* [1, c], *Ayagma Zhargalova* [2, d], *Ziqi Tong* [2, e], *Egor Rozhnov* [1, f], *Gleb Drach* [2, g], *Alexey Morozov* [2, h]

[1] Novosibirsk State Technical University, 20 Prospekt K. Marksa, Novosibirsk, 630073, Russian Federation
[2] Bauman Moscow State Technical University, 5/1 2nd Baumanskaya St., Moscow, 105005, Russian Federation

[a] https://orcid.org/0000-0002-1664-5351, pjui@mail.ru; [b] https://orcid.org/0000-0001-9244-225X, ivancivskij@corp.nstu.ru;
[c] https://orcid.org/0000-0002-5811-5519, martynova@corp.nstu.ru; [d] https://orcid.org/0000-0002-6251-1004, azhargalova@bmstu.ru;
[e] https://orcid.org/0009-0008-6174-3234, tongziqi29@gmail.com; [f] https://orcid.org/0009-0003-6779-0553, EgoRozhnov@yandex.ru;
[g] https://orcid.org/0009-0005-7618-2896, drach1254@gmail.com; [h] https://orcid.org/0009-0002-1846-7592, 2809322@gmail.com

ARTICLE INFO

Article history:
Received: 01 January 2026
Revised: 14 January 2026
Accepted: 14 February 2026
Available online: 15 March 2026

Keywords:
Millstone mechanism
Dynamic model
Moment of inertia
Runge–Kutta method
Support force
Power consumption
Energy efficiency
Parameter optimization

Funding
This study was supported by NSTU grant (project No. TP-PTM-1_26).

Acknowledgements
The research was carried out using the equipment of the Engineering Center “Design and Production of High-Tech Equipment”.

ABSTRACT

Introduction. Millstone mills hold a special place among the grinding equipment used in the food industry, as they produce flour with a high content of biologically valuable grain components through the repeated action of working surfaces on the processed material. However, existing industrial designs of millstone units are characterized by significant energy consumption caused by the high moments of inertia of the rotating millstones. In the context of the ongoing drive toward import substitution and modernization of grain processing enterprises, there is a need to develop new energy-efficient equipment that meets modern requirements for productivity and specific energy consumption. Despite the long history of millstone mill application, the issues of selecting rational inertial-mass characteristics and design parameters of the rotating millstone and their influence on the dynamic parameters of the drive and support forces remain insufficiently studied. ***The purpose of this study*** is to reduce the power consumption of a millstone mill by developing a dynamic model of the mechanism and determining rational design and kinematic parameters of the unit. **Methods.** Based on *D'Alembert's* principle, a system of differential equations of motion was formulated for a shaft with a disk (millstone), taking into account the eccentricity of the rotation axis relative to the geometric axis of the millstone. The law of motion was determined by numerical integration using the fourth-order *Runge–Kutta* method with variation of the moments of inertia of the rotating millstone (25.185–40.388 kg·m²) and driving torques (250–500 N·m). Support forces were then calculated by solving matrix equations of static equilibrium , using the previously obtained kinematic characteristics. Finally, a parametric analysis of the influence of inter-supports distances and manufacturing accuracy on the magnitude of support forces was carried out. **Results and Discussion.** It was found that reducing the moment of inertia of the rotating millstone from 40.388 to 25.185 kg·m² leads to a decrease in shaft acceleration time to steady-state rotational speed from 12.2–15.7 s to 7.2–10.0 s and to a reduction in maximum support forces at the most loaded support from 1,000–1,700 N to 600–1,000 N over the driving torque range of 300–500 N·m. It was shown that the rational inter-support distance is 0.58 m, and the permissible displacement of the rotation axis relative to the geometric axis of the millstone should not exceed 0.5–1.0 mm, at which the maximum support force does not exceed 360–700 N. For the proposed design with a millstone moment of inertia of 25.185 kg·m² and a driving torque of 280–300 N·m, the power consumption at the drive shaft was 10.5 kW, which is 50% lower than that of the industrial mill *AVR 6-890* (21 kW) at a comparable capacity of 490 kg/h. The obtained results demonstrate the feasibility of structural lightening of the rotating millstone as an effective strategy for improving the energy efficiency of millstone mills.

For citation: Podgornyj Y.I., Ivancivsky V.V., Martynova T.G., Zhargalova A.D., Ziqi Tong, Rozhnov E.E., Drach G.A., Morozov A.A. Dynamic modeling and selection of rational parameters for a millstone mill mechanism to reduce energy consumption. *Obrabotka metallov (tekhnologiya, oborudovanie, instrumenty) = Metal Working and Material Science*, 2026, vol. 28, no. 1, pp. 193–206. DOI: 10.17212/1994-6309-2026-28.1-193-206. (In Russian).

*** Corresponding author**
Podgornyj Yuriy I., D.Sc. (Engineering), Professor
Novosibirsk State Technical University,
20 Prospekt K. Marksa,
630073, Novosibirsk, Russian Federation
Tel: +7 383 346-17-79,**e-mail:** pjui@mail.ru

Introduction

Millstone mills rank among the oldest and most widespread types of grinding equipment, with a history of utilization spanning several millennia [1, 2]. Notwithstanding the introduction of roller mills and hammer crushers since the mid-nineteenth century, millstone installations have retained their significance in the flour milling industry owing to the specific mechanism of repeated action of the working surfaces on the grain, which ensures the production of flour with a high content of biologically valuable constituents [3, 4]. Contemporary trends in the food processing sector, driven by increasingly stringent requirements for both end-product quality and equipment energy efficiency, have stimulated scientific research aimed at improving the design of millstone units [5, 6].

From an engineering standpoint, the working elements of grinding machines undergo rotary motion at peripheral velocities ranging from 4 to 100 m/s and above, while the dynamic loads on individual assemblies and on the machine as a whole increase substantially with rising throughput [7, 8–18]. This circumstance imposes heightened demands on the dynamic models employed during the design of equipment components and assemblies. In particular, for millstone mills the inertial characteristics of the rotating millstone are of paramount importance, as the moment of inertia of industrial units may reach 40–50 kg·m^2 [19, 20]. The considerable inertia of the millstone causes the predominant share of the consumed power to be expended not on the useful grinding of grain but on sustaining the rotary motion of the massive working element.

The dynamics of rotating components in mechanisms and machines, including problems of determining the laws of motion, support reaction forces, and energy characteristics of drive systems, have been treated in detail in classical works on the theory of mechanisms and machines [21–24]. Analytical and numerical methods for investigating dynamic models of cyclic machines have been advanced in the studies of *Vul'fson* [25] and *Dresig* [26], as well as in a number of publications devoted to the kinematic and dynamic analysis of process equipment [27–29]. However, the aforementioned investigations predominantly focus on general methodological approaches, whereas the problem of selecting rational inertial and structural parameters of the millstone working element from the standpoint of energy consumption minimization has not received adequate attention.

Issues of flour milling equipment design and operation, including millstone assemblies, are addressed in a number of specialized publications [1, 3, 30–32]. Recommendations for the management of technological processes at flour milling enterprises, incorporating data on working element loads, are presented in [33, 34]. Problems of technical diagnostics and modernization of flour mill equipment are discussed in [35, 36]. Nonetheless, the available literature lacks systematic investigations linking the moments of inertia of the rotating millstone to the dynamic characteristics of the drive, support reaction forces, and the total energy consumption of the installation.

The challenge of import substitution of equipment for grain storage and processing enterprises constitutes a topical issue and is included in the state program "Development of Agriculture and Regulation of Agricultural Product, Raw Material and Food Markets" (code 01.05 "Technical and Technological Modernization, Innovative Development") [37, 38]. In this context, the development of domestic millstone mills with reduced energy consumption is of both scientific and practical interest.

An analysis of the published data allows the following contradiction to be articulated: on the one hand, a massive millstone ensures stable, uniform rotation and effective grain comminution; on the other hand, its substantial moment of inertia constitutes the primary source of excessive energy consumption. Resolving this contradiction necessitates the development of a scientifically grounded approach to determining the minimum requisite inertial characteristics of the millstone while ensuring the specified technological parameters of the grinding process.

Thus, ***the purpose of the present study*** is to reduce the power consumption of a millstone mill through the development of a dynamic model of the mechanism and the determination of rational kinematic design parameters of the installation.

To achieve the stated objective, the ***following tasks*** were formulated:

− to develop a dynamic model of the millstone unit mechanism accounting for the eccentricity of the rotating millstone's axis of rotation;

− to determine the law of motion of the shaft with the millstone under variation of inertial and reaction force parameters;

− to establish rational design dimensions for the bearing spans of the shaft;

− to determine permissible manufacturing accuracy values for the rotation axis of the rotating millstone relative to its geometric axis;

− to calculate the power consumption for the design with the determined rational parameters and to compare it with the industrial prototype.

Methods

Prototype description and problem formulation

The industrial millstone mill *AVR 6-890* was selected as the prototype for comparative analysis, featuring the following specifications: rotating millstone speed – 350 min^{-1}, millstone diameter – 890 mm, electric motor power – 22 kW, throughput – 490 kg/h. The driving torque at the specified throughput is $\boldsymbol{M}$ = 643 N·m, while the useful resistance torque is 22.5 N·m [33], which constitutes merely 3.5 % of the total driving torque. Consequently, the predominant share of consumed energy is expended on overcoming the inertia of the rotating millstone, whose moment of inertia for this installation equals 40.388 kg·m^2 (determined using the *KOMPAS-3D* graphics package).

This ratio of useful to total torques provided the rationale for formulating the problem of creating a design with reduced millstone inertia.

Schematic of the proposed design

A modified design of the millstone unit is proposed (Fig. 1), comprising a stationary millstone **1**, a rotating millstone **2**, transfer levers **3** and **4**, intermediate brackets **5** and **6**, an adjusting screw **7**, a handwheel with nut **8**, a V-belt drive **9**, and an electric motor **10**. The fundamental distinction of the proposed design lies in the structural lightweighting of the rotating millstone while preserving its functional characteristics. A detailed description of the unit operation is presented in [19].

Computational scheme and equations of motion

For the mathematical description of the unit behavior, a computational scheme was formulated, as shown in Fig. 2. The drive shaft of the millstone unit is represented by the $\boldsymbol{OZ}$ axis, on which the millstone, modeled as a disk, is mounted. The center of mass of the millstone (point $\boldsymbol{C}$), due to unavoidable manufacturing

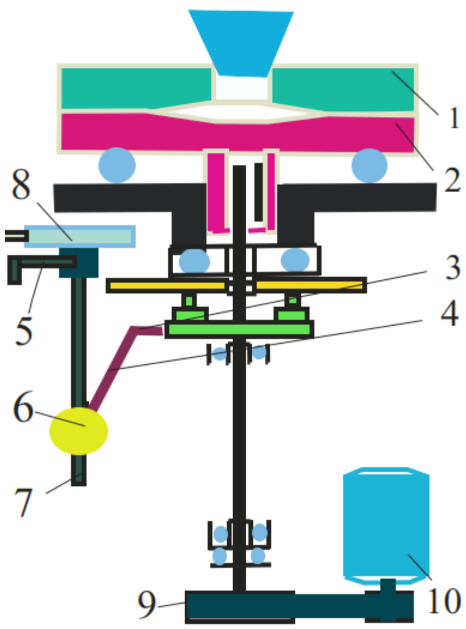

Fig. 1. Schematic diagram of the proposed millstone unit design:
1 – stationary millstone; 2 – rotating millstone; 3, 4 – transfer levers; 5, 6 – intermediate brackets; 7 – screw; 8 – handwheel with nut; 9 – V-belt drive; 10 – electric motor

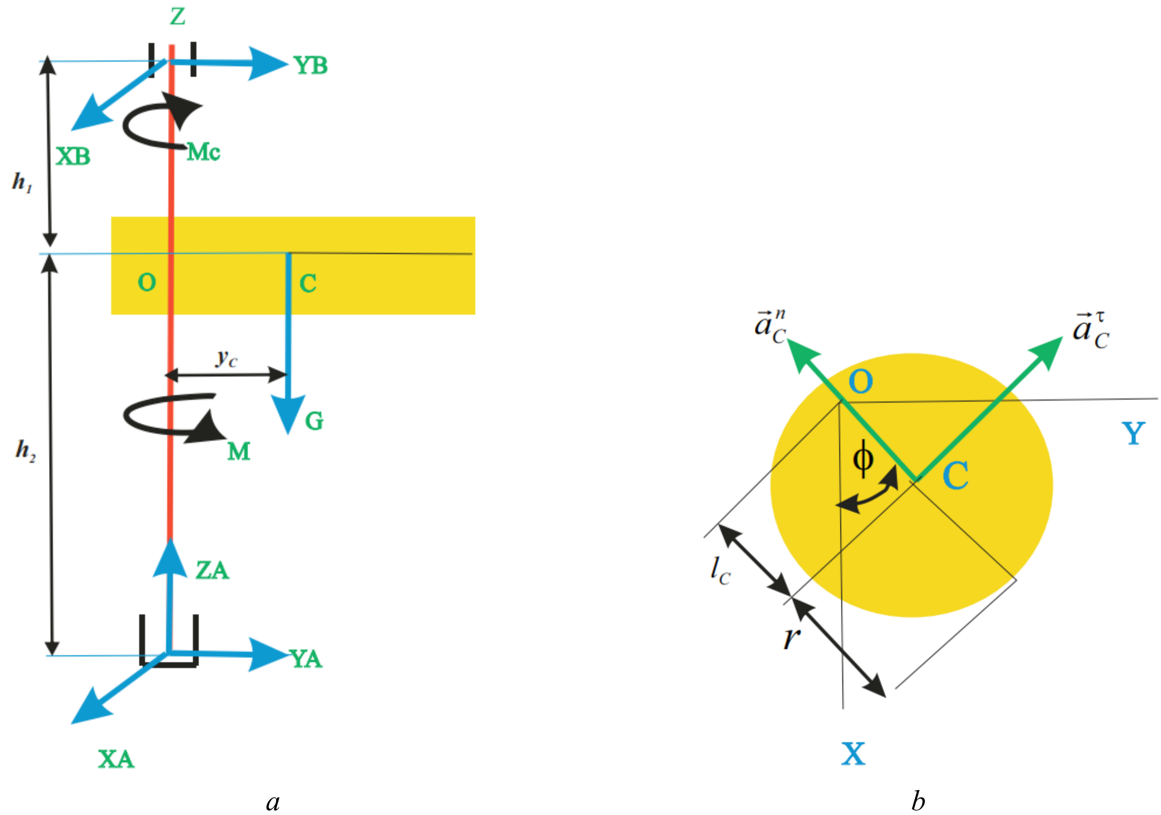

Fig. 2. Computational scheme of the millstone unit:
a – arrangement of supports and applied forces; *b* – components of the center of mass acceleration

tolerances, is offset from the rotation axis (point ***O***) by a distance l_c. The reaction forces at supports ***A*** and ***B*** in the ***XY*** plane are denoted as ***XA***, ***YA***, ***XB***, ***YB*** (Fig. 2, *a*). Fig. 2, *b* shows the normal and tangential components of the total acceleration of the center of mass.

The active forces acting in the system include the gravitational force ***G***, a force couple with driving torque ***M***, and a force couple with resistance torque M_c. Since the rotation axis of the millstone is perpendicular to its plane of symmetry, it constitutes a principal axis of inertia at point ***O*** of intersection with the said plane; consequently, the products of inertia vanish.

Applying *d'Alembert's* principle, the system of equations of motion is written in the form:

$$\begin{aligned}
&XA + XB + m \cdot xc \cdot \omega^2 + m \cdot yc \cdot \varepsilon = 0;\\
&YA + YB + m \cdot yc \cdot \omega^2 - m \cdot xc \cdot \varepsilon = 0;\\
&YA \cdot (h_1 + h_2) + YB \cdot h_2 - m \cdot g \cdot yc = 0;\\
&-XB \cdot h_2 - XA(h_1 + h_2) + m \cdot g \cdot xc = 0;\\
&ZA - G = 0;\\
&J_{OZ} \cdot \varepsilon = M - M_C = 0,
\end{aligned} \tag{1}$$

The first five equations of system (1) permit the determination of the unknown reaction forces at the supports; the vertical component ***ZA* = *G*** is independent of the disk's law of motion. The sixth equation defines the law of motion of the shaft with the millstone and, for the convenience of numerical integration, is recast in the form:

$$J_{OZ} \cdot \ddot{\varphi} = M - \nu \cdot \dot{\varphi}^2, \tag{2}$$

where J_{OZ} is the moment of inertia of the disk (millstone) about the rotation axis (kg·m²); *M* is the driving torque (N·m); ν is the viscous resistance coefficient, taken as 0.2 [15]; $\dot{\varphi}$ and $\ddot{\varphi}$ are the angular velocity and angular acceleration, respectively.

Numerical solution method

Differential equation (2) was solved numerically by the fourth-order *Runge–Kutta* method with a constant step size (the *rkfixed* function in the *Mathcad* environment). The program listing is presented in Fig. 3, where the following notation is adopted: *rkfixed* is the built-in *ODE* (ordinary differential equation) solver based on the *Runge–Kutta* method; the initial condition vector specifies the initial angle of rotation and the initial angular velocity; **0** and ***T*** are the bounds of the time integration interval; ***N*** is the number of discretization points; ***D*** is the right-hand side vector of the *ODE* system reduced to *Cauchy* normal form.

$$J_{OZ} \cdot \ddot{\varphi} = M - \nu \cdot \dot{\varphi}^2;$$
$$T := 50 N := T \cdot 100;$$
$$D(t,u) := \begin{bmatrix} u_1 \\ \dfrac{M}{J_{OZ}} - \dfrac{\nu}{J_{OZ}} \cdot \left(u_1{}^2\right) \end{bmatrix};$$
$$\alpha := rkfixed\left[\begin{pmatrix} 0 \\ 0 \end{pmatrix}, 0, T, N, D\right];$$
$$t := \alpha^{\langle 0 \rangle} \varphi := \alpha^{\langle 1 \rangle} \omega := \alpha^{\langle 2 \rangle};$$
$$\omega_{ust} := \sqrt{\frac{M}{\nu}}.$$
$$\varepsilon = \frac{M}{J_{OZ}} - \frac{\nu}{J_{OZ}} \cdot \omega^2$$

Fig. 3. Program listing for the numerical solution of differential equation (2) by the *Runge–Kutta* method

The solution yields a matrix of dimension (***N*** + 1) × 3: the first column contains discrete time values, the second – values of the angle of rotation, and the third – values of the angular velocity. The angular acceleration is computed by numerical differentiation of the obtained solution.

Determination of support reaction forces

For the computation of support reaction forces, the system comprising the first four equations of (1) (excluding the fifth and sixth) was expressed in matrix form:

$$A := \begin{matrix} 1 & 0 & 1 & 0 \\ 0 & 1 & 0 & 1 \\ 0 & h_1 + h_2 & 0 & h_2 \\ -h_2 & 0 & h_1 + h_2 & 0 \end{matrix}; \qquad B := \begin{bmatrix} -m \cdot xc \cdot \omega^2 - m \cdot yc \cdot \varepsilon \\ -m \cdot yc \cdot \omega^2 + m \cdot xc \cdot \varepsilon \\ m \cdot g \cdot yc \\ -m \cdot g \cdot xc \end{bmatrix} \tag{3}$$

where ***A*** is a fourth-order square coefficient matrix whose elements are determined by the unit direction cosines of the reaction forces and the moment arms of the forces about the support points (distances h_1 and h_2, see Fig. 2, *a*); ***X*** is the sought vector of reaction forces $(XA, YA, XB, YB)^T$; ***B*** is the right-hand side vector incorporating inertial terms.

The reduced mass in matrix ***B*** was determined from the relation $\boldsymbol{m = 2J_{OZ} / D^2}$, where ***J_OZ*** is the moment of inertia of the disk (millstone) with the shaft about the vertical axis; ***D*** is the disk diameter [13]; $\boldsymbol{x_c} = l_c \cdot \cos(\varphi)$; $\boldsymbol{y_c} = l_c \cdot \sin(\varphi)$; **ω** is the angular velocity of rotation of the shaft with the disk; and **ε** is the angular acceleration of the shaft with the disk (see Fig. 2, *b*).

The matrix equation (3) was solved at each time step using the algorithm whose listing is presented in Fig. 4: for each value of loop index ***i*** (***i***∈0…*N*), $\boldsymbol{X}^{<i>} = A^{-1} \cdot B^{<i>}$ was computed. The resultant reaction force moduli were determined as the geometric sum of the corresponding components.

$$
X := \left|
\begin{array}{l}
A \leftarrow \begin{bmatrix} 1 & 0 & 1 & 0 \\ 0 & 1 & 0 & 1 \\ 0 & h_1 + h_2 & 0 & h_2 \\ -h_1 & 0 & h_1 + h_2 & 0 \end{bmatrix} \\
fori \in 0 \cdot\cdot N \\
\quad \left| B^{\langle i \rangle} \leftarrow \begin{bmatrix} -\cos(\varphi_i)\cdot(\omega_i)^2 - \sin(\varphi_i)\cdot\varepsilon_i \\ -\sin(\varphi_i)\cdot(\omega_i)^2 + \cos(\varphi_i)\cdot\varepsilon_i \\ g\cdot\sin(\varphi_i) \\ -g\cdot\cos(\varphi_i) \end{bmatrix} \right. \\
X^{\langle i \rangle} \leftarrow A^{-1}\cdot B^{\langle i \rangle} \\
X^T
\end{array}
\right.
$$

$$i := 0 \cdot\cdot N;$$

$$XA_i := X_{1,0}; YA_i := X_{i.1};$$

$$RA_i := \sqrt{(XA_i)^2 + (YA_i)^2};$$

$$XB_i := X_{1,2}; YB_i := X_{1,3};$$

$$RB_i := \sqrt{(XB_i)^2 + (YB_i)^2}.$$

Fig. 4. Program listing for computing support forces

Varied parameters

The parametric study was conducted for four discrete values of the rotating millstone moment of inertia: 40.388 kg·m² (corresponding to the industrial prototype *AVR 6-890*), 35.351 kg·m², 30.314 kg·m², and 25.185 kg·m². The driving torque was varied over the range 250–500 N·m in increments of 50 N·m. The bearing spans h_1 and h_2 were varied from 0.40 to 0.80 m in increments of 0.08 m. The eccentricity of the rotation axis l_c was assigned values of 0.5, 1.5, 2.5, 3.5, and 5.0 mm.

Results and Discussion

Law of motion of the shaft with the millstone

In the first stage of the investigation, the kinematic characteristics of the shaft with the disk were determined by solving differential equation (2) . The primary output parameters analyzed were the steady-state angular velocity $\boldsymbol{\omega}_{st}$, the maximum angular acceleration $\boldsymbol{\varepsilon}_{max}$, and the run-up time $\boldsymbol{t}_r$ to attainment of the steady-state state.

For the industrial prototype (moment of inertia $\boldsymbol{J}_{OZ}$ = 40.388 kg·m^2, driving torque $\boldsymbol{M}$ = 250 N·m), it was established (Fig. 5) that the steady-state angular velocity is $\boldsymbol{\omega}_{st}$ = 35.357 s^{-1} (corresponding to a rotational speed of $\boldsymbol{n}$ = 337.6 min^{-1}), the run-up time is 16.089 s, and the maximum angular acceleration is 6.67 s^{-2}. Upon increasing the driving torque to $\boldsymbol{M}$ = 300 N·m (Fig. 6), the steady-state angular velocity rose to $\boldsymbol{\omega}_{st}$ = 38.642 s^{-1} ($\boldsymbol{n}$ = 369 min^{-1}), the run-up time decreased to 15.6 s, and the maximum acceleration increased to 7.2 s^{-2}. Thus, an increase in the driving torque by 50 N·m yielded an acceleration increment of 0.53 s^{-2}, a run-up time reduction of 0.4 s, and an increase in the steady-state rotational speed of 19 min^{-1}.

Influence of the moment of inertia on the run-up time

For a comprehensive assessment of the effect of inertial characteristics on the drive dynamics, a series of four calculation variants was carried out at discrete values of the millstone moment of inertia (25.185,

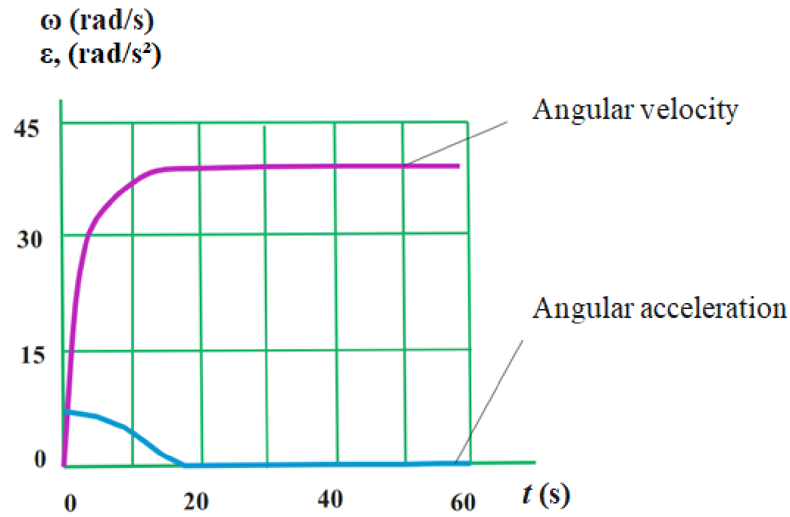

Fig. 5. Time histories of the angular velocity and angular acceleration of the shaft with the disk for the *AVR 6-890* mill at $\boldsymbol{M}$ = 250 N·m and $\boldsymbol{J_{oz}}$ = 40.388 kg·m²

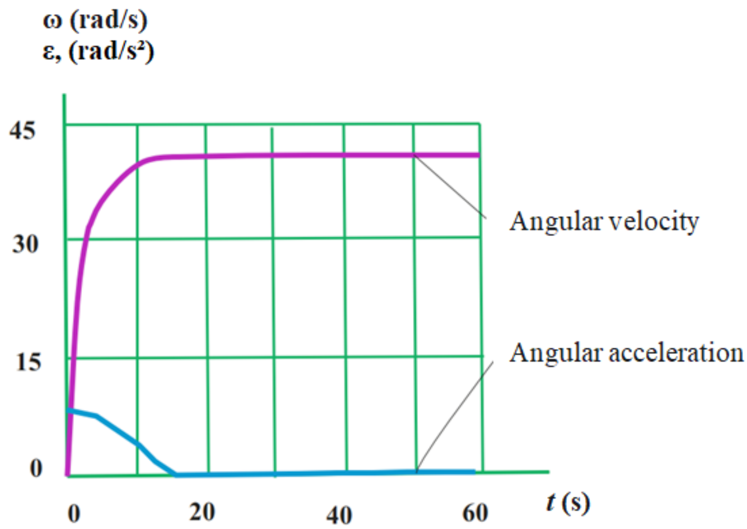

Fig. 6. Time histories of the angular velocity and angular acceleration of the shaft with the disk for the *AVR 6-890* mill at $\boldsymbol{M}$ = 300 N·m and $\boldsymbol{J_{oz}}$ = 40.388 kg·m²

30.314, 35.351, and 40.388 kg·m²) and driving torques from 300 to 500 N·m in increments of 50 N·m. The results are presented in Fig. 7 as dependences of the run-up time $\boldsymbol{t_r}$ on the driving torque magnitude.

Analysis of the obtained curves reveals that across the entire investigated parameter range, the minimum run-up time corresponds to the design with the lowest moment of inertia, $\boldsymbol{J_{oz}}$ = 25.185 kg·m². For this configuration, the time to reach steady-state angular velocity is 7.2–10.0 s depending on the driving torque magnitude, whereas for the industrial prototype ($\boldsymbol{J_{oz}}$ = 40.388 kg·m²) the corresponding value lies in the range of 12.2–15.7 s. The run-up time reduction of 35–41 % is indicative of a substantial improvement in the dynamic characteristics of the drive system upon decreasing the millstone moment of inertia.

It should be noted that the dependence of the run-up time on the driving torque exhibits a nonlinear character with a decreasing rate of reduction at $\boldsymbol{M}$ > 400 N·m, which is attributable to the increase in dissipative losses at higher angular velocities. This pattern provides a rational basis for limiting the range of driving torque values, thereby avoiding an unjustified increase in drive power.

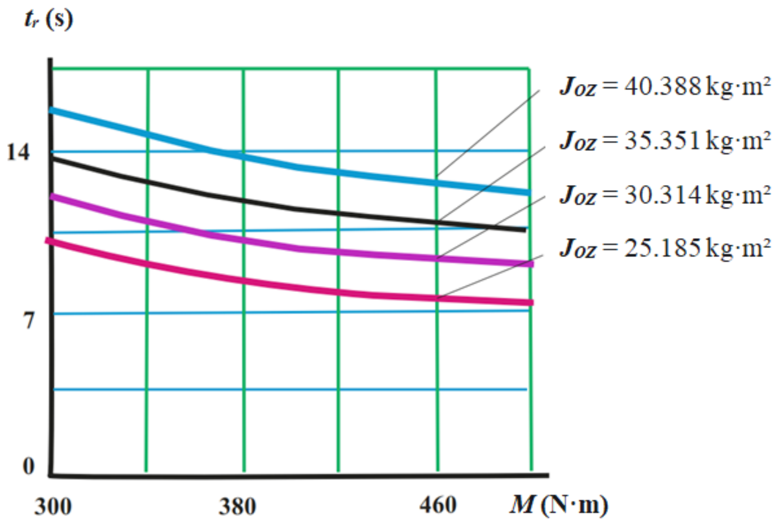

Fig. 7. Dependence of the shaft run-up time on the driving torque for different values of the rotating millstone moment of inertia: J_{oz} = 25.185 kg·m²; J_{oz} = 30.314 kg·m²; J_{oz} = 35.351 kg·m²; J_{oz} = 40.388 kg·m²

Support reaction forces

In the second stage of the investigation, following the determination of kinematic characteristics, the reaction forces at supports ***A*** and ***B*** were calculated (see expressions (3) and the listing in Fig. 4). Fig. 8 presents one of the representative calculation variants at J_{oz} = 25.185 kg·m² and ***M*** = 300 N·m. It was established that the reaction forces at support ***B*** exceed those at support ***A*** by more than a factor of two, which is attributable to the location of the millstone on the cantilever section of the shaft. For this reason, the subsequent parametric analysis was focused on the characteristics of the most heavily loaded support ***B***.

The results of the forces calculations at support ***B*** for the four moment-of-inertia variants are presented in Fig. 9. The lowest reaction forces values across the entire driving torque range (300–500 N·m) are observed for the design with J_{oz} = 25.185 kg·m²: the reaction forces amount to 600–1,000 N. For the industrial prototype (J_{oz} = 40.388 kg·m²), the reaction forces at support ***B*** under analogous conditions reach 1,000–1,700 N. The 40–42 % reduction in support reaction forces accompanying the 37.7 % decrease in the millstone moment of inertia constitutes a significant result with practical implications for ensuring the service life of bearing assemblies.

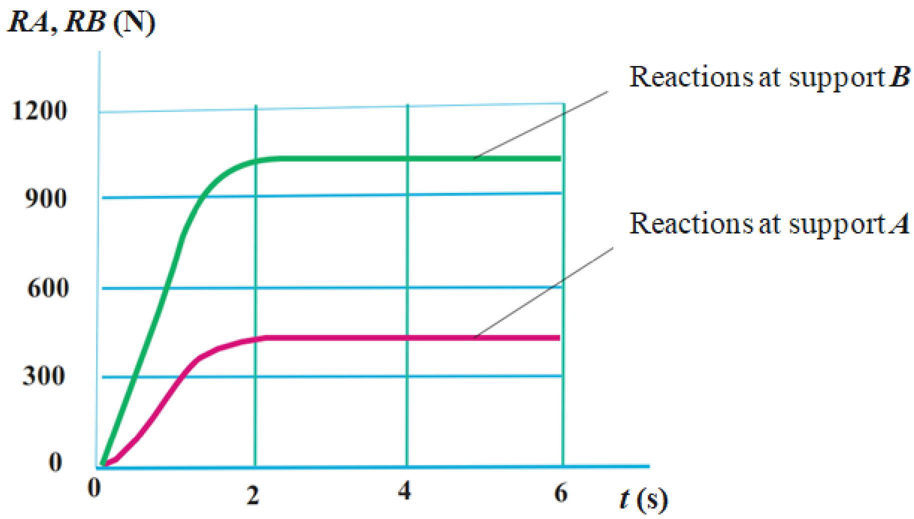

Fig. 8. Time histories of the support forces in supports ***A*** and ***B*** at J_{oz} = 25.185 kg·m² and ***M*** = 300 N·m

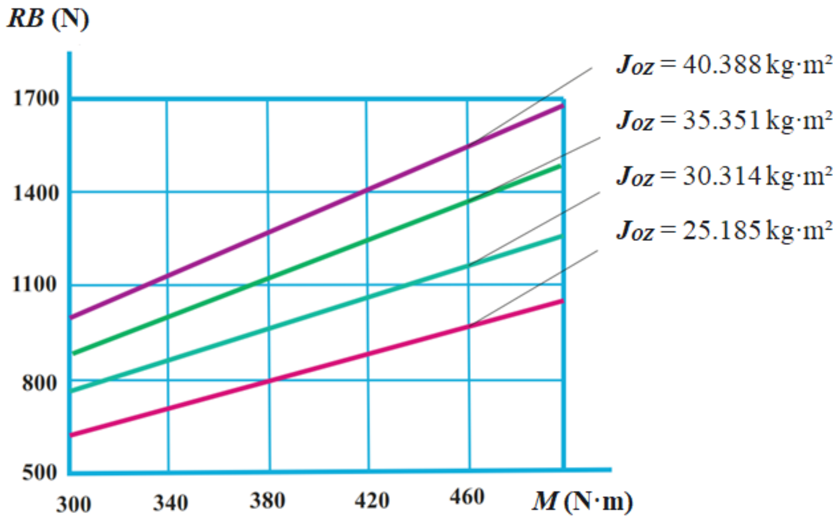

Fig. 9. Dependence of the support forces in support ***B*** on the driving torque for different values of the rotating millstone moment of inertia: J_{oz} = 25.185 kg·m²; J_{oz} = 30.314 kg·m²; J_{oz} = 35.351 kg·m²; J_{oz} = 40.388 kg·m²

Influence of inter-support distances on support reaction forces

To establish rational overall dimensions of the installation along its height, a parametric study of the effect of distances h_1 and h_2 (see Fig. 2, *a*) on the reaction force at support ***B*** was conducted. The distances were varied from 0.40 to 0.80 m in increments of 0.08 m. The results are presented in Fig. 10.

Analysis of the plots reveals that the nature of the influence of the two investigated parameters differs markedly: an increase in distance h_2 by 0.4 m leads to an increase in the reaction force at support ***B*** of 122 N, whereas an analogous increase in distance h_1 causes a decrease in the force of 105 N. The curves intersect at a distance value of approximately 0.58 m, which corresponds to the minimum total loading of the support assembly and may be recommended as a rational design solution.

Physically, this pattern is explained by the fact that increasing h_1 (the distance from the lower support to the millstone plane) leads to a redistribution of the bending moment between the supports with a reduction in the share borne by support ***B***, whereas increasing h_2 (the distance from the upper support to the millstone plane) increases the moment arm of the inertial forces acting about support ***B***.

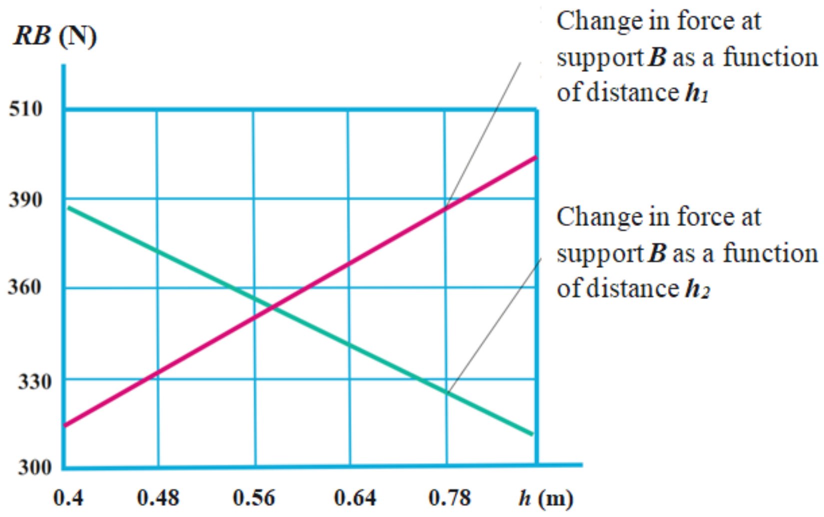

Fig. 10. Effect of inter-support distances h_1 and h_2 on the reaction force in support ***B***

Influence of manufacturing accuracy on support force

The practical significance of the dynamic analysis results is largely governed by the sensitivity of support reaction force to manufacturing tolerances. Accordingly, an assessment was performed of the effect of the displacement of the millstone rotation axis relative to its geometric axis (eccentricity l_c) on the reaction force at the most heavily loaded support ***B***. The eccentricity values were varied from 0.5 to 5.0 mm.

The results (Fig. 11) reveal a pronounced dependence: at a manufacturing accuracy of 0.5 mm, the reaction force at support ***B*** is 360 N, whereas at an offset of 5.0 mm it increases to 3,000 N – i.e., by more than a factor of eight. This dependence is virtually linear in character, which enables the prediction of dynamic load levels for intermediate eccentricity values.

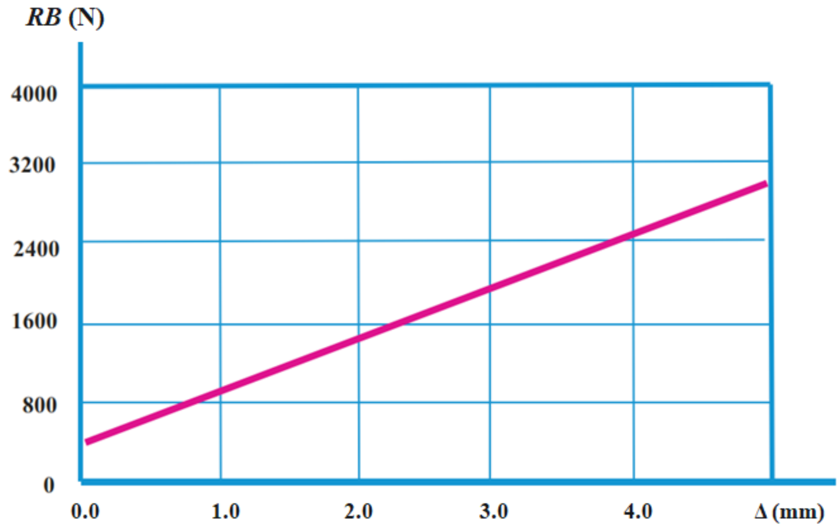

Fig. 11. Dependence of the support forces in support ***B*** on the eccentricity of the millstone rotation axis relative to its geometric axis

In light of the obtained results, it is recommended to ensure that the alignment accuracy of the rotation axis with the geometric axis of the millstone be maintained within 0.5–1.0 mm, for which the support force remains within 360–700 N and can be reliably accommodated by standard bearing assemblies without degradation of their service life.

Energy efficiency of the proposed design

Based on the totality of the conducted investigations, the rational parameters of the proposed millstone mill design were determined: rotating millstone moment of inertia – 25.185 kg·m²; driving torque – 280–300 N·m; bearing spans – $h_1 = h_2 = 0.58$ m; permissible eccentricity – not exceeding 1.0 mm.

Under the specified parameters, the power consumption at the millstone drive shaft was $P = 10.5$ kW, whereas for the industrial prototype *AVR 6-890* the corresponding value is 21 kW. Thus, the proposed design provides a 50 % reduction in power consumption while maintaining a throughput of 490 kg/h. This substantial energy saving is attributable to a synergistic effect: the 37.7 % reduction in the millstone moment of inertia decreases not only the inertial component of the torque but also the dissipative losses proportional to the angular velocity.

The obtained result is consistent with the theoretical tenets of cyclic machine dynamics [25, 26], according to which the energy expenditure for accelerating and sustaining the motion of a rotating working element is directly proportional to its moment of inertia. It should be noted, however, that a reduction in millstone mass necessitates monitoring the stability of the grinding process, as diminished inertia may lead to increased sensitivity of the rotational speed to load pulsations. This issue warrants further experimental investigation using actual grain batches of varying conditions.

Conclusion

In the present study, a dynamic model of the millstone mill mechanism was developed and a comprehensive parametric analysis was performed with the aim of determining rational kinematic design parameters that ensure reduced energy consumption. The principal results and conclusions are as follows.

Based on *D'Alembert's* principle, a system of equations of motion for the shaft with the rotating millstone was formulated, accounting for the eccentricity of the rotation axis. The second-order differential equation was solved by the fourth-order *Runge–Kutta* method, and the support forces were determined at each time step through the solution of a matrix equation. The developed dynamic model can be employed at the design stage of millstone installations of varying throughput capacities.

It was established that reducing the moment of inertia of the rotating millstone from 40.388 to 25.185 kg·m² (by 37.7 %) results in a decrease in the shaft run-up time to steady-state rotational speed from 12.2–15.7 s to 7.2–10.0 s (by 35–41 %) over the driving torque range of 300–500 N·m.

It was demonstrated that reducing the millstone moment of inertia ensures a decrease in the maximum forces at the most heavily loaded support $\boldsymbol{B}$ from 1,000–1,700 N (for the prototype) to 600–1,000 N (for the proposed design), representing a 40–42 % reduction, which has a beneficial effect on the service life of the bearing assemblies.

Rational bearing spans of $\boldsymbol{h_1} = \boldsymbol{h_2} = 0.58$ m were determined, and permissible manufacturing accuracy values for the rotation axis of the rotating millstone were established, with the eccentricity not exceeding 0.5–1.0 mm, corresponding to a reaction force at support B of no more than 360–700 N.

For the proposed design with the selected parameters ($\boldsymbol{J_{OZ}} = 25.185$ kg·m², $\boldsymbol{M} = 280$–300 N·m), the power consumption at the millstone drive shaft was 10.5 kW, which is 50 % lower than that of the industrial mill *AVR 6-890* (21 kW) while maintaining a throughput of 490 kg/h.

A promising direction for further research is the experimental verification of the developed dynamic model on a full-scale prototype, as well as the investigation of the influence of variable technological loads on the stability of the grinding process at reduced millstone moment of inertia.

References

1. Demskii A.B., Boriskin M.A., Tamarov T.V., Chernolikhov A.S. *Oborudovanie dlya proizvodstva muki i krupy: spravochnik* [Equipment for the production of flour and groats. Handbook]. Moscow, Agropromizdat Publ., 1990. 352 p.

2. Merko I.T. *Tekhnologiya mukomol'nogo i krupyanogo proizvodstva* [Technology of flour milling and groat production]. Moscow, Agropromizdat Publ., 1985. 288 p.

3. Butkovskii V.A., Ptushkina G.E. *Tekhnologicheskoe oborudovanie mukomol'nogo proizvodstva* [Technological equipment of flour milling production]. Moscow, Khleboprodukty Publ., 1999. 208 p.

4. Egorov G.A. *Tekhnologiya pererabotki zerna* [Grain processing technology]. Moscow, Kolos Publ., 1977. 376 p.

5. Temirov M.M. Importozameshchenie i puti razvitiya mashinostroeniya dlya ego resheniya [Import substitution and ways of developing mechanical engineering for its solution]. *Khleboprodukty = Khleboproducty*, 2015, no. 7, pp. 12–13.

6. Temirov M.M. Sovremennoe rossiiskoe oborudovanie dlya predpriyatii khraneniya i pererabotki zerna [Modern Russian equipment for grain storage and processing enterprises]. *Khleboprodukty = Khleboproducty*, 2016, no. 7, pp. 10–11.

7. Dresig H., Holzweißig F. *Dynamics of machinery: Theory and applications*. 2nd ed. Berlin, Heidelberg, Springer-Verlag, 2010. 554 p. ISBN 978-3-540-89939-6. DOI: 10.1007/978-3-540-89940-2.

8. Uicker J.J., Pennock G.R., Shigley J.E. *Theory of machines and mechanisms*. 5th ed. New York, Oxford University Press, 2017. 960 p. ISBN 978-0-19-060415-3.

9. Zhu Y., Luo Z., Wang H., Zhang Z. Numerical investigation of particle segregation in millstone systems: An enhanced quantification approach. *Chemical Engineering Research and Design*, 2025, vol. 223, pp. 238–252. DOI: 10.1016/j.cherd.2025.08.021.

10. Zhu Y., Luo Z., Wang H., Zhou Q., Zhang Z. Air-induced segregation of micron-scale particles in a vertical roller mill. *Minerals Engineering*, 2026, vol. 239, p. 110114. DOI: 10.1016/j.mineng.2026.110114.

11. Podgornyj Yu.I., Skeeba V.Yu., Kirillov A.V., Pushnin V.N., Erokhin I.A., Kornev D.Yu. *Modelirovanie nesushchikh sistem tekhnologicheskikh mashin* [Modeling of the technological machines support systems]. *Obrabotka metallov (tekhnologiya, oborudovanie, instrumenty) = Metal Working and Material Science*, 2014, no. 2 (63), pp. 91–99.

12. Podgornyj Yu.I., Skeeba V.Yu., Martynova T.G., Maksimchuk O.V. *Issledovanie i vybor parametrov pri proektirovanii tekhnologicheskikh mashin* [Analysis and choice of parameters in designing technological machines]. Novosibirsk, NSTU Publ., 2020. 260 p. ISBN 978-5-7782-4177-0.

13. Podgornyj Yu.I., Martynova T.G., Skeeba V.Yu. *Sintez tekhnologicheskikh mashin. Raschet i konstruirovanie* [Synthesis of technological machines. calculation and design]. Novosibirsk, NSTU Publ., 2023. 240 p. ISBN 978-5-7782-4912-7. DOI: 10.17212/978-5-7782-4912-7.

14. Flores P., Souto A.P., Marques F. The first fifty years of the Mechanism and Machine Theory: Standing back and looking forward. *Mechanism and Machine Theory*, 2018, vol. 125, pp. 8–20. DOI: 10.1016/j.mechmachtheory.2017.11.017.

15. Eckhardt H.D. *Kinematic design of machines and mechanisms*. 1st ed. New York, McGraw-Hill, 1998. 620 p. ISBN 0070189536. ISBN 978-0070189539.

16. Erdman A.G., Sandor G.N. *Mechanism design: analysis and synthesis*. 4th ed. Upper Saddle River, NJ, Pearson, 2001. 688 p. ISBN 0130408727. ISBN 978-0130408723.

17. Zhu B., Zhang X., Zhang H., Liang J., Zang H., Li H., Wang R. Design of compliant mechanisms using continuum topology optimization: a review. *Mechanism and Machine Theory*, 2012, vol. 143, p. 103622. DOI: 10.1016/j.mechmachtheory.2019.103622.

18. Vulfson I. *Dynamics of cyclic machines*. Cham, Springer International Publ., 2015. 390 p. ISBN 978-3-319-12633-3. DOI: 10.1007/978-3-319-12634-0.

19. Podgornyj Y.I., Skeeba V.Y., Martynova T.G. *Tekhnologicheskoe oborudovanie: raschet i proektirovanie* [Technological equipment: calculation and design]. Novosibirsk, NSTU Publ., 2024. 107 p. ISBN 978-5-7782-5308-7.

20. Antipov S.T., Kretov I.T., Ostrikov A.N. *Mashiny i apparaty pishchevykh proizvodstv*. V 2 kn. Kn. 1 [Machines and apparatus of food production. In 2 bk. Bk. 1]. Moscow, Vysshaya shkola Publ., 2001. 703 p.

21. Artobolevskii I.I. *Teoriya mekhanizmov i mashin: uchebnik dlya vtuzov* [Theory of mechanisms and machines]. 4th ed. Moscow, Nauka Publ., 1988. 640 p. ISBN 5-02-013810-X.

22. Levitskii N.I. *Teoriya mekhanizmov i mashin* [Theory of mechanisms and machines]. 2nd ed. Moscow, Nauka Publ., 1990. 592 p. ISBN 5-02-014188-7.

23. Frolov K.V. *Teoriya mekhanizmov i mashin* [Theory of mechanisms and machines]. Moscow, Vysshaya shkola Publ., 1987. 496 p.

24. Bat' M.I., Dzhanelidze G.Yu., Kel'zon A.S. *Teoreticheskaya mekhanika v primerakh i zadachakh*. T. 1 [Theoretical mechanics in examples and problems. Vol. 1]. Moscow, Nauka Publ., 1990. 672 p. ISBN 5-02-014450-9.

25. Vul'fson I.I. *Dinamika tsiklovykh mashin* [Dynamics of cyclic machines]. St. Petersburg, Politekhnika Publ., 2013. 425 p. ISBN 978-5-7325-1024-9.

26. Dresig H., Vul'fson I.I. *Dynamik der Mechanismen*. Wien, Springer-Verlag, 1989. 328 p. ISBN 978-3-7091-9036-4. DOI: 10.1007/978-3-7091-9035-7.

27. Podgornyj Y.I., Skeeba V.Yu., Martynova T.G., Pechorkina N.S., Skeeba P.Yu. Kinematic analysis of crank-cam mechanism of process equipment. *IOP Conference Series: Materials Science and Engineering*, 2018, vol. 327, p. 042080. DOI: 10.1088/1757-899X/327/4/042080.

28. Podgornyj Y.I., Skeeba V.Yu., Kirillov A.V., Martynova T.G., Skeeba P.Yu. Motion laws synthesis for cam mechanisms with multiple follower displacement. *IOP Conference Series: Materials Science and Engineering*, 2018, vol. 327, p. 042079. DOI: 10.1088/1757-899X/327/4/042079.

29. Fomin A., Paramonov M. Synthesis of the four-bar double-constraint mechanisms by the application of the Grubler's method. *Procedia Engineering*, 2016, vol. 150, pp. 871–877. DOI: 10.1016/j.proeng.2016.07.034.

30. Kulak V.G., Maksimchuk B.M., Chakar A.P. *Mukomol'nye zavody na komplektnom oborudovanii* [Flour mills on packaged equipment]. Moscow, Kolos Publ., 1984. 263 p.

31. Katsnel'son M.U., Demskii A.B., Dub M.D. *Tekhnicheskoe diagnostirovanie oborudovaniya mukomol'nykh zavodov* [Technical diagnostics of flour mill equipment]. Moscow, Kolos Publ., 1984. 220 p.

32. Maevskaya S.L., Labutina O.A. *Kolichestvenno-kachestvennyi uchet zerna i zernoproduktov* [Quantitative and qualitative accounting of grain and grain products]. Moscow, DeLi print Publ., 2003. 296 p.

33. Berestnev E.V., Petrichenko V.E., Petrichenko V.V. *Rekomendatsii po organizatsii i vedeniyu tekhnologichesk-ogo protsessa na mukomol'nykh predpriyatiyakh* [Recommendations for the organization and management of the technological process at flour milling enterprises]. 2nd ed. Moscow, DeLi Publ., 2020. 368 p.

34. Egorov G.A. Pererabotka zerna v muku [Grain processing into flour]. *Spravochnik po torgovle zernom*. Ch. 2 [Handbook on grain trade. Pt. 2]. Moscow, Spetstekhnika Publ., 1999. 320 p.

35. Fomin A., Dvornikov L., Paramonov M., Jahr A. To the theory of mechanisms subfamilies. *IOP Conference Series: Materials Science and Engineering*, 2016, vol. 124, p. 012055. DOI: 10.1088/1757-899X/124/1/012055.

36. Makarov E. *Inzhenernye raschety v Mathcad 14* [Engineering calculations in Mathcad 14]. St. Petersburg, BHV-Peterburg Publ., 2007. 592 p.

37. Seal C.J., Brownlee I.A. Whole grains and health, evidence from observational and intervention studies. *Cereal Chemistry*, 2010, vol. 87 (2), pp. 167–174.

38. Febles C.I., Arias A., Hardisson A., Rodríguez-Alvarez C., Sierra A. Phytic acid level in wheat flours. *Journal of Cereal Science*, 2002, vol. 36 (1), pp. 19–23.

Conflicts of Interest

The authors declare no conflict of interest.